CERN – EUROPEAN ORGANIZATION FOR NUCLEAR RESEARCH

CTF3-Note-106
(tbts, bpm, commissioning)

Commissioning of inductive BPMs in the TBTS probe beam line

A. Palaia
Uppsala University

Abstract

The probe beam line of the Two-beam Test Stand at CTF3 is equipped with 5 inductive Beam Position Monitors. Here we discuss their calibration and resolution measurements carried on during the summer 2012.

Geneva, Switzerland

(15th July 2013)

1 Introduction

The probe beam line of the Two-beam Test Stand (TBTS) at CTF3 is equipped with 5 inductive Beam Position Monitors (BPM) [1], placed as shown in Fig. 1, two upstream and three downstream of the accelerator structure, the last one is in the spectrometer line. They have been originally designed and optimised for the CTF3 drive beam, which consists of trains of electron bunches of a variable length between 1.2 μs and 140 ns, with peak current between 4 A and 28 A. Nevertheless they have been as well installed as diagnostics for the probe beam, which consists of 0.6 to 150 ns long trains of electron bunches, with 0.13 A maximum peak current [2].

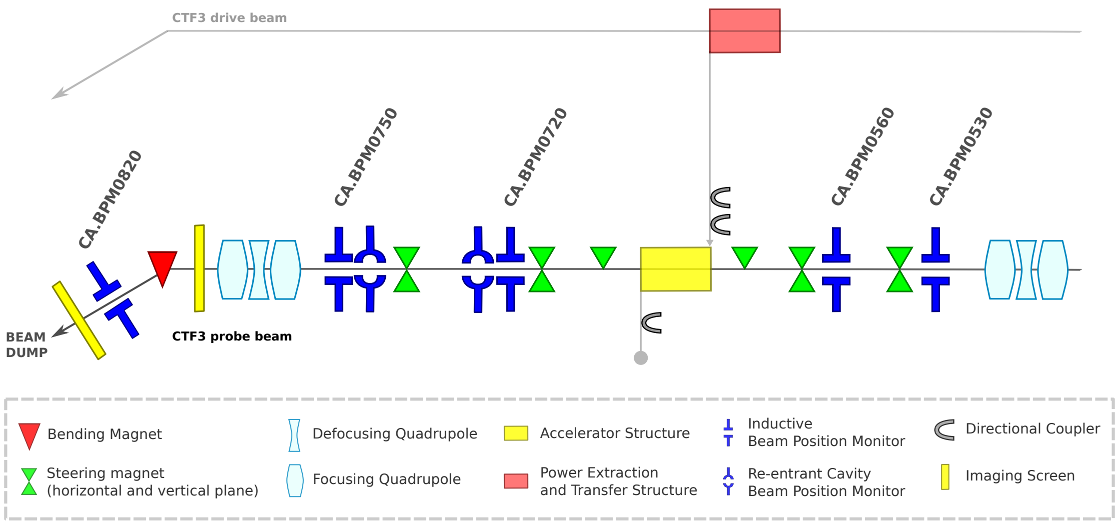

Figure 1: Sketch of the probe beam line of the Two-Beam Test Stand at the CLIC Test Facility 3. Five inductive Beam Position Monitors are installed in the beam line, two upstream and three downstream of the accelerator structure, the last one being in the spectrometer line. Only the names of the hardware relevant to this paper are reported in the drawing.

Each BPM consists of two parts: an inductive pick-up installed in the beam line and a front-end electronics which receives, combines and amplifies the signals from the pick-up before they are sent to the digitisers. A first mechanical and electrical calibration of the pick-ups was performed on a test bench [3] before their installation in the beam line. Once installed, they have to be calibrated together with their front-end electronics and read-out system (cables and digitisers). To this purpose a procedure was developed which simulates the beam current and its position by means of a synthetic external current signal sent to the front-end electronics [4]. The calibration obtained in this way is available in the CTF3 control system and used in the control software during normal operations. We will refer to this calibration as *standard calibration* to distinguish it from the *beam-based calibration* carried out during the CTF3 2012 run which is described and discussed in this paper.

This paper is organised as follows. At first we describe the main characteristics of the pick-up and the read-out electronics. Afterwards we discuss the calibration of the current and position signals. Finally, we describe the methodology used for the measurement of the spatial resolution and we present and discuss the results.

2 Hardware set-up

Every BPM consists of an inductive pick-up and a front-end electronics. Each pick-up consists of 8 copper electrodes assembled around the beam line axis, as shown in Fig. 2. Every electrode picks up a signal whose amplitude is proportional to the beam current and to the distance of the beam from it. Such signal is then amplified in a toroidal current transformer assembled on an electronic board shown in Fig. 3 and installed on the pick-up itself. At this point the signals from the 8 electrodes are summed by twos as sketched in Fig. 2: the signals from the two rightmost electrodes are summed to form the H_+ signal whereas the leftmost are summed to form the H_- signal. In the same fashion, the signals from the two uppermost and the two lowermost electrodes are summed to form the V_+ and V_- signals, respectively. Finally, these four signals are sent to an active hybrid circuit which produces one sum Σ signal, proportional to the beam current, and two difference Δ signals, proportional to the beam position on the horizontal and vertical planes, and defined as follows:

$$\Sigma = H_+ + H_- + V_+ + V_- \tag{1}$$

$$\Delta H = \frac{H_+ - H_-}{\Sigma} \tag{2}$$

$$\Delta V = \frac{V_+ - V_-}{\Sigma} \tag{3}$$

which define a right-handed reference system for the BPM. The difference $H_+ - H_-$ is proportional to the distance of the beam from the centre of the BPM on the horizontal plane and it is divided by the sum signal Σ in order make the ΔH signal independent on the beam current. Similarly, the difference ΔV is proportional to the distance of the beam from the centre of the BPM on the vertical plane, irrespective of the beam current.

The Σ, ΔH and ΔV signals are finally amplified and sent over about 30 m of coaxial cable to an ADC, sampled at 192 MHz and made available in the control system. An amplification stage located in the front-end electronics has two different gains, which can be remotely set, of about 44 dB or 24 dB for the Δ signals and 27 dB or 7 dB for the Σ signals. Due to the low probe beam current of about 1.3 A usually the maximum amplification is chosen, which is also the case for the measurements discussed in this paper.

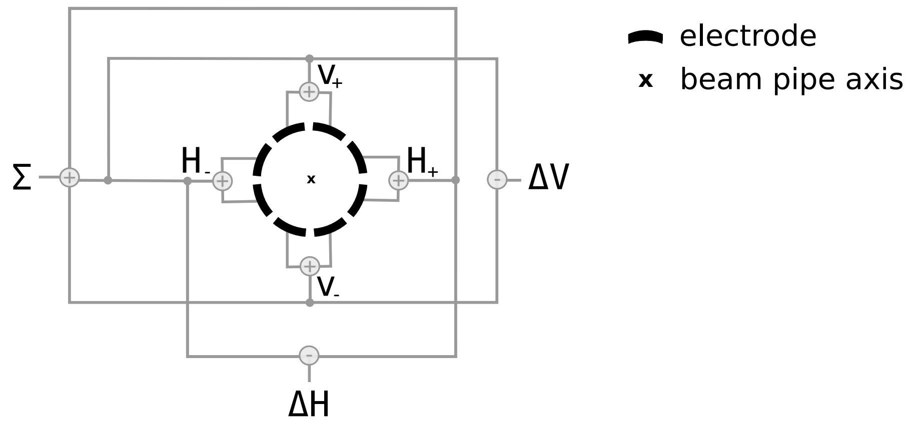

Figure 2: Inductive peak-up and scheme of signal treatment. 8 electrodes are assembled around the beam line axis. The signals picked up by each one of them are summed by two and then again combined and subtracted to produce one sum Σ and two difference Δ signals.

3 Calibration

Here we discuss the calibration of current Σ and position Δ signals, based on direct measurement of beam current and position. Because one of the main goal of the TBTS is the study of beam before and after the acceleration in a CLIC prototype structure, our main interest is to measure relative changes of the beam current and position along the beam line or, in other words, we are mainly interested in the resolution of this measurement [5]. This is especially true for the current signals, whose resolution is of bigger relevance than its closeness to the true value, i.e. its accuracy. That applies as well to the position signals although in this case we have lower tolerance of their accuracy because of the control of the beam orbit needed to transport the beam in an accelerator structure with a geometrical aperture of only 6 mm.

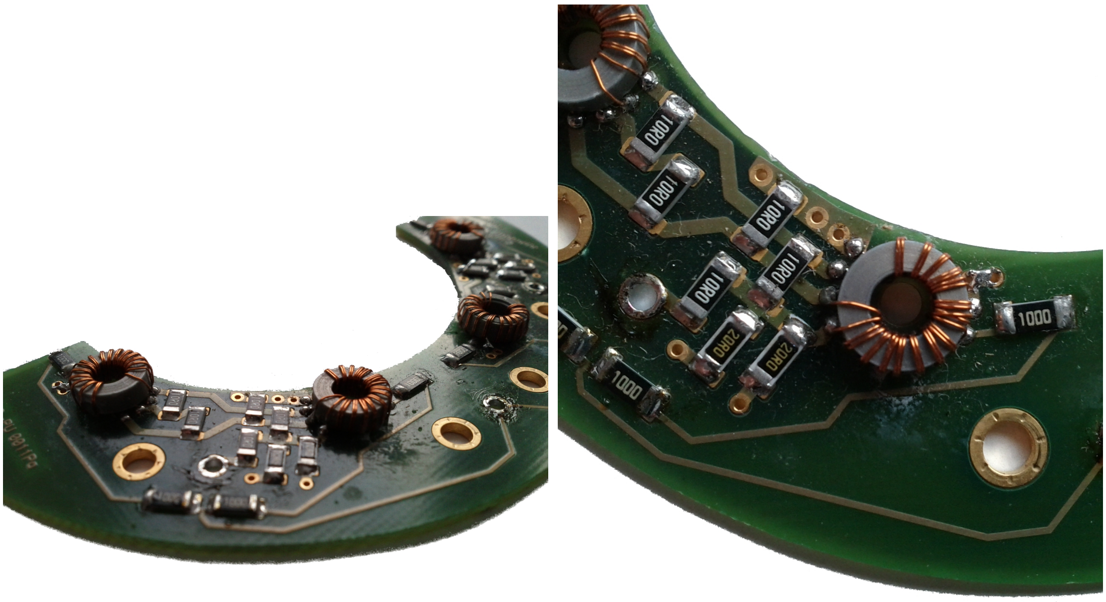

(a) (b)

Figure 3: (a) D-shaped PCB on which the current transformers are mounted. Two PCB of this type are mounted on every BPM. (b) A closer view of one current transformer. A pin connected to one of the electrodes is inserted in the toroid on which are visible the secondary windings of the current transformer.

3.1 Current

The beam-based calibration of the current signals consists of the following two steps:

1. optimisation of the beam transport by maximising all Σ signals;
2. equalisation of all Σ signals with respect to first BPM in the beam line (`CA.BPM0530`).

The calibration is based on the analysis of 345 signals, each one corresponding to a 100 ns long bunch-train measured on the Σ signals and a total charge of 14 nC measured by the wall current monitor installed upstream of the TBTS. The ratios between the magnitude of the Σ signals and the magnitude of the signal of the first BPM for the same bunch-train are shown in Fig. 4 and their mean values and standard deviations are summarised in Table 1. They show that the response of all BPMs to the same beam current varies within 2.5%. The calibration coefficients are finally calculated multiplying such values by the scale factor of 0.150 ± 0.008 AV^{-1}and are summarised in Table 1.

Because no diagnostics specifically dedicated to the measurements of the beam current is installed in the TBTS, the overall scale factor is taken from the standard calibration of `CA.BPM0530` and is 0.150 AV^{-1}, which therefore defines the accuracy of our calibration. To that conversion factor we associate an uncertainty given by the standard deviation of the noise in the Σ signal of `CA.BPM0530` of 0.008 AV^{-1}.

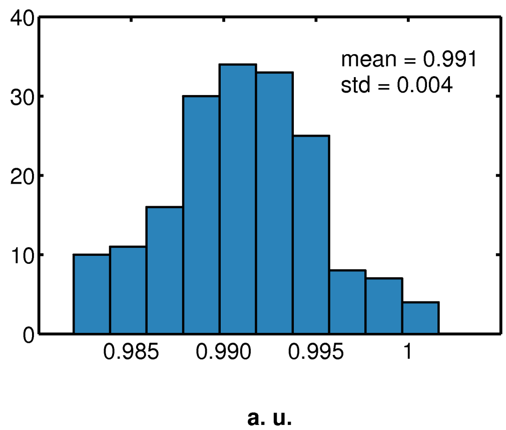

(a) `CA.BPM0560`

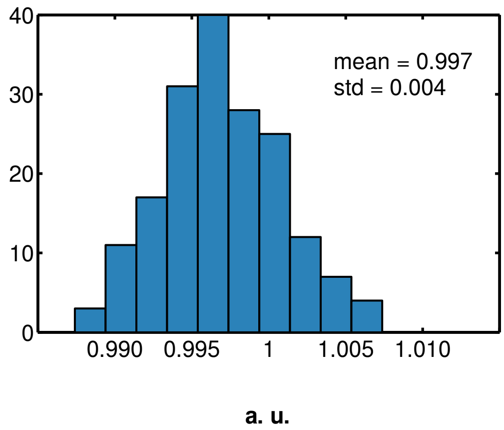

(b) `CA.BPM0720`

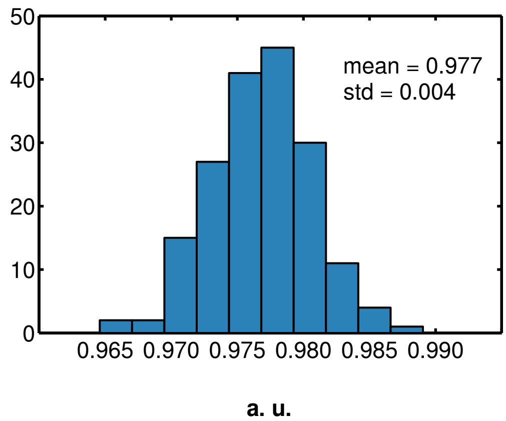

(c) `CA.BPM0750`

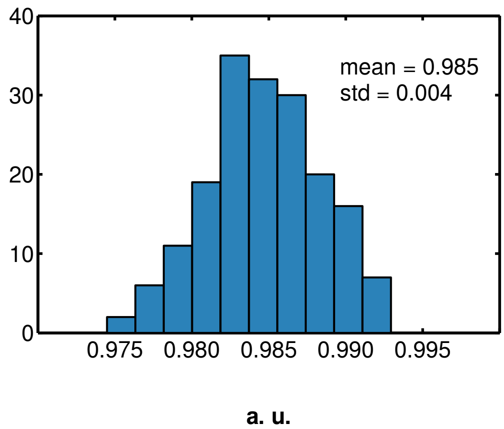

(d) `CA.BPM0820`

Figure 4: Histograms of the magnitude of the Σ signals with respect to the first BPM in the beam line (`CA.BPM0530`).

Table 1: Calibration coefficients for the Σ signals of all inductive BPM and their ratio with respect to the first BPM in the beam line (`CA.BPM0530`).

BPM name	ratio	calibration coeff. [A V^{-1}]
`CA.BPM0530`	1	0.150 ± 0.009
`CA.BPM0560`	0.991 ± 0.004	0.151 ± 0.009
`CA.BPM0720`	0.997 ± 0.004	0.150 ± 0.009
`CA.BPM0750`	0.977 ± 0.004	0.154 ± 0.009
`CA.BPM0820`	0.985 ± 0.004	0.152 ± 0.009

3.2 Position

The calibration of the Δ signals is obtained measuring how their amplitude changes while the beam is steered with an upstream corrector on both the horizontal and vertical planes. Such change is then compared with the expected position of the beam at each BPM estimated on the basis of the measurement of the position of the beam centroid on the imaging screen `CA.MTV0790` at the end of the straight section of the beam line (see Fig. 1). Because of the fact that the imaging screen `CA.MTV0790` intercepts the beam before the spectrometer line, no calibration of the Δ signals of the last BPM (`CA.BPM0820`) was performed.

The position of the beam centroid on the screen is calculated by means of a fit of a 2D-Gaussian to the beam spot image. We assumed all longitudinal coordinates from the mechanical drawing [6] and subsequent survey of the beam line [6] which are summarised in Table 2, and the calibration of the corrector magnet as documented in [7]. For this measurement all the correctors and quadrupoles in the beam line were not powered such that the beam trajectory was ballistic along the beam line.

The plots in Fig. 5 show the correlation between the amplitude of the BPM signals and the position of the beam measured on the imaging screen, for both the horizontal and vertical plane. The position of the beam at i-th BPM is estimated multiplying the position of the beam centroid measured on the screen by a factor l_i/r, where l_i is the distance between the steering magnet and the i-th BPM and r is the distance between the steering magnet and the screen. All longitudinal distances between the steerer and the BPMs and screen are summarised in Table 2. The slope of the straight lines fitting the experimental points in Fig. 5 multiplied by the factor l_i/r represent the calibration coefficients for each BPM which are summarised in Table 3.

It is worth noting that the BPM response is linear within the range of about

Table 2: Longitudinal distances between the corrector magnet `CA.DHG/DVG0385` at the end of CALIFES and the BPMs listed.

BPM name	[mm]	ratio
`CA.BPM0530`	3778.5	0.31
`CA.BPM0560`	4877.2	0.40
`CA.BPM0720`	8974.0	0.74
`CA.BPM0750`	10576.0	0.87
`CA.MTV0790`	12179.1	1

Table 3: Calibration coefficients for the 4 inductive BPMs in the straight section of the probe beam line in TBTS.

BPM name	horizontal [mm]	vertical [mm]
`CA.BPM0530`	5.57 ± 0.41	5.96 ± 1.15
`CA.BPM0560`	5.58 ± 0.31	5.95 ± 0.72
`CA.BPM0720`	5.98 ± 0.29	6.02 ± 0.31
`CA.BPM0750`	5.77 ± 0.28	5.71 ± 0.30

± 2.5 mm spanned by the beam and even beyond such range. Some non-linearities were measured when the beam was displaced by more than 15 mm in case of low amplification of the BPM signals and by more than 8 mm in case of high amplification. The cause of the limited linear range in the response in the case of high amplification of the signals was identified in the saturation of the amplifier in the front-end electronics.

4 Resolution

The BPM resolution is defined as the standard deviation of the distribution of the residuals given by comparing the beam position measured at one BPM with the beam position expected at the same BPM. The latter is estimated on the basis of the beam position measured at two other BPMs, under the assumption that the beam trajectory is a straight line and that the distances between BPMs are known. To this purpose all quadrupoles in the beam line were not powered during the measurements. That was not the case for corrector magnets whose effect is a systematic shift of the distributions of residuals as it is the effect of any errors in the assumption of the BPM distances. In both cases the standard deviation of the distribution of the residuals in unaffected.

The methodology just described was followed to measure the resolution of the BPMs in the straight section of the probe beam line, i.e. the two BPMs before and the two after the accelerating structure (Fig. 1). Consider for instance BPM `CA.BPM0530`, the first in the probe beam line (see Fig. 1). First of all we calculate the beam position expected at this BPM given the measurements of two other BPMs in the line. As there are 4 BPMs, we can rely on the measurements of the second and the third (`CA.BPM0560` and `CA.BPM0720`), the second and the fourth (`CA.BPM0560` and `CA.BPM0750`) or the third and the fourth (`CA.BPM0720` and `CA.BPM0750`). After that we calculate the residual given by comparing the estimated beam position with the measured one.

Because we are interested in resolving small changes of the beam trajectory along a single bunch-train, we apply the methodology outlined above taking into account the beam position sample-by-sample along a BPM trace (the sampling frequency is 192 MHz). The distributions of the residuals for each BPM are shown in Fig. 6 for the horizontal plane and in Fig. 7 for the vertical plane, with a result on the order of 100 micrometre.

The same methodology can be applied averaging the beam position over the whole bunch-train, i.e. averaging over the whole BPM trace. The corresponding distributions of residuals are shown in Fig. 8 for the horizontal plane and in Fig. 9 for the vertical plane. The standard deviations of the distributions of the residuals calculated this way result smaller by a factor $\sqrt{18} = 4.2$ than the ones calculated with the sample-by-sample method, which is consistent with the fact that the beam position is averaged over the whole bunch-train of 100 ns corresponding to 18 samples. Nevertheless we note that the distribution calculated with this second methodology includes outliers which have no physical meaning but can be due, for example, to alignment errors between different BPM signals. Therefore we fit a Gaussian function to the distributions - which is only marginally affected by the outliers - and we consider its standard deviation the resolution of our measurements.

The resolutions measured with the two methodologies discussed is summarised in Table 4. The results show that in general the best resolution is obtained when the residuals are calculated taking into account at least one BPM next to the one whose resolution is being measured, for instance the first two plus one of the remaining when measuring the resolution of one of the first two, or the second two plus one of the first two when measuring the resolution of one of the second ones. Moreover, we noticed that vertical resolution is always worse than the horizontal resolution. This difference is not understood.

5 Conclusions

We discussed the beam-based calibration and the measurement of the spatial resolution of the inductive BPMs installed in the TBTS probe beam line at CTF3. The beam-based calibration has to be considered complementary to the standard calibration which is normally used in the control software. Our beam-based calibration as well as the measured resolution are used in the off-line data analysis.

For what concerns the Σ signals, which are proportional to the beam current, we focused on their relative calibration, i.e. all the signals are calibrated relatively to the first BPM in the beam line. This is because no redundant measurement is available to measure the beam current that can be compared with the BPM signals. We calculated the calibration coefficients for all BPMs with a relative uncertainty or precision of about 6%.

The calibration of the Δ signals, which are proportional to the beam position, is based on the measurements of the beam centroid on an imaging screen installed before the spectrometer line while the beam is steered with an upstream magnet. The accuracy of this calibration is therefore dependent on the calibration of the imaging screen and on the accuracy of the measurement of the longitudinal coordinates BPMs and imaging screen in the beam line. The calibration coefficients calculated for the four BPMs in the straight section of the beam line are given with a precision of about 7%.

Finally, we measured the spatial resolution of the four BPMs in the straight section of the beam line, on the basis of the beam-based calibration of their Δ signals. To the purpose, two different methodology were used. The first one takes into account the beam position along a single bunch-train whereas the second methodology is based on the beam position averaged over the whole bunch-train. The resolution calculated with the second method is better than the one calculated with the first method. Moreover, we found that irrespective of the methodology used, the vertical resolution is always worse than the horizontal resolution.

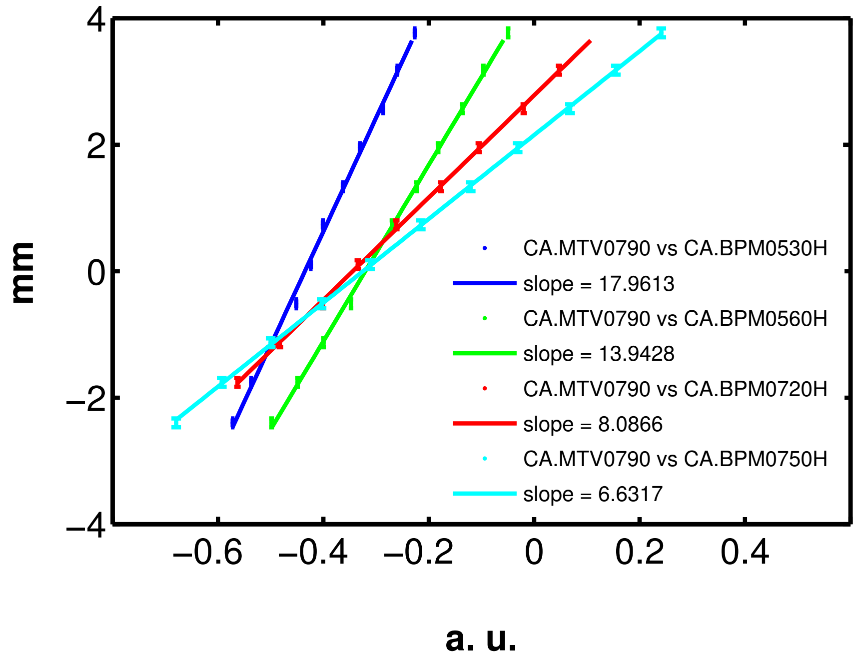

(a)

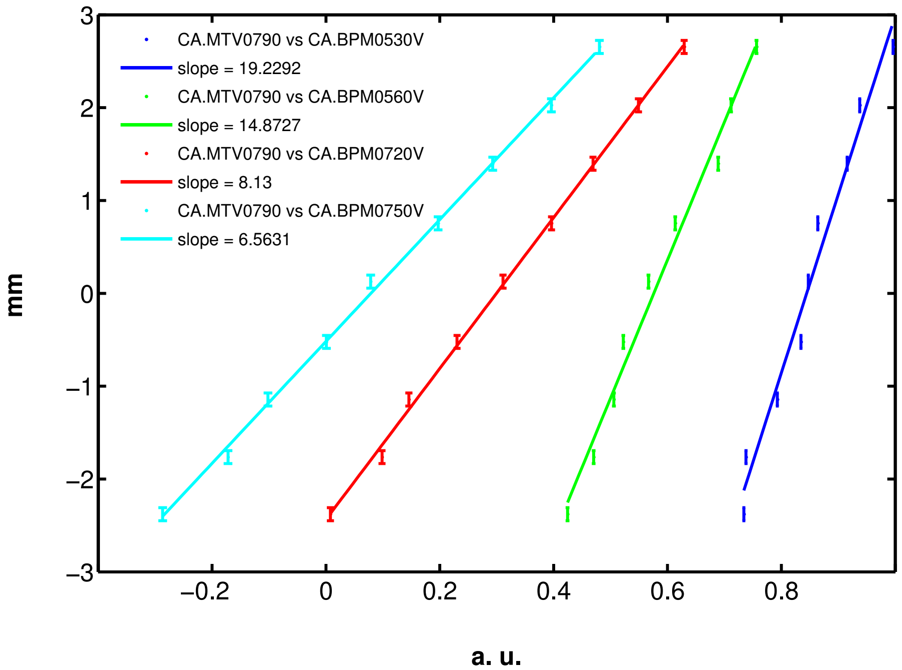

(b)

Figure 5: Correlation between the amplitude of the BPM signals and the position of the beam measured on the imaging screen downstream of all BPMs. The BPMs taken into account are the four ones in the straight section of the beam line and the measurements shown here refer to both (a) the horizontal (b) and the vertical plane.

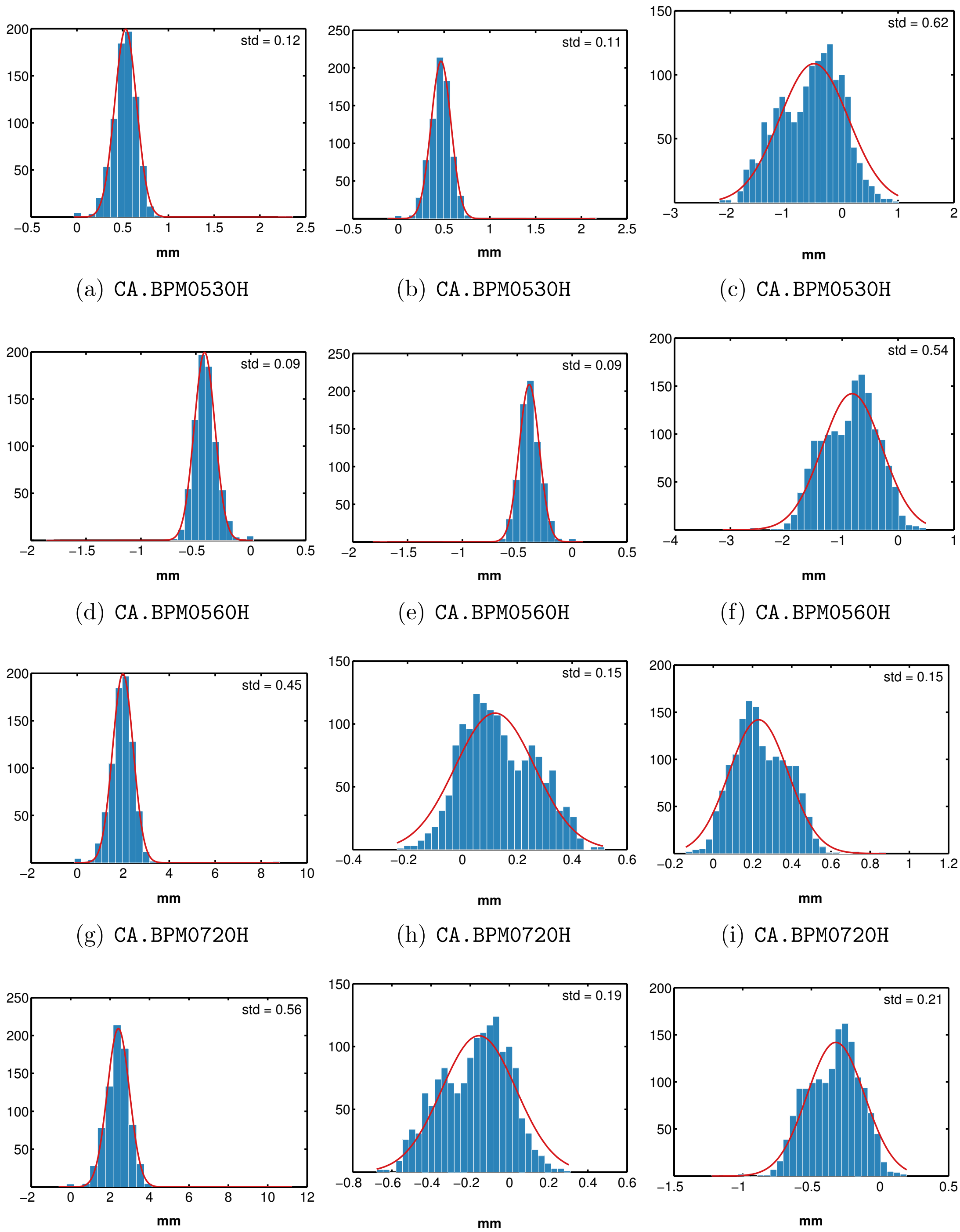

(a) `CA.BPM0530H` (b) `CA.BPM0530H` (c) `CA.BPM0530H`

(d) `CA.BPM0560H` (e) `CA.BPM0560H` (f) `CA.BPM0560H`

(g) `CA.BPM0720H` (h) `CA.BPM0720H` (i) `CA.BPM0720H`

(j) `CA.BPM0750H` (k) `CA.BPM0750H` (l) `CA.BPM0750H`

Figure 6: Resolution of the horizontal probe beam BPMs calculated taking the beam position sample-by-sample along a BPM trace. Histograms of residuals between expected and measured beam position at each probe beam BPM based on the measurements of the BPM listed in the last column of Table 4 (data from 18 June 2012). The standard deviation `std` quoted at the top right of each histogram is the width of the Gaussian function fit to each distribution.

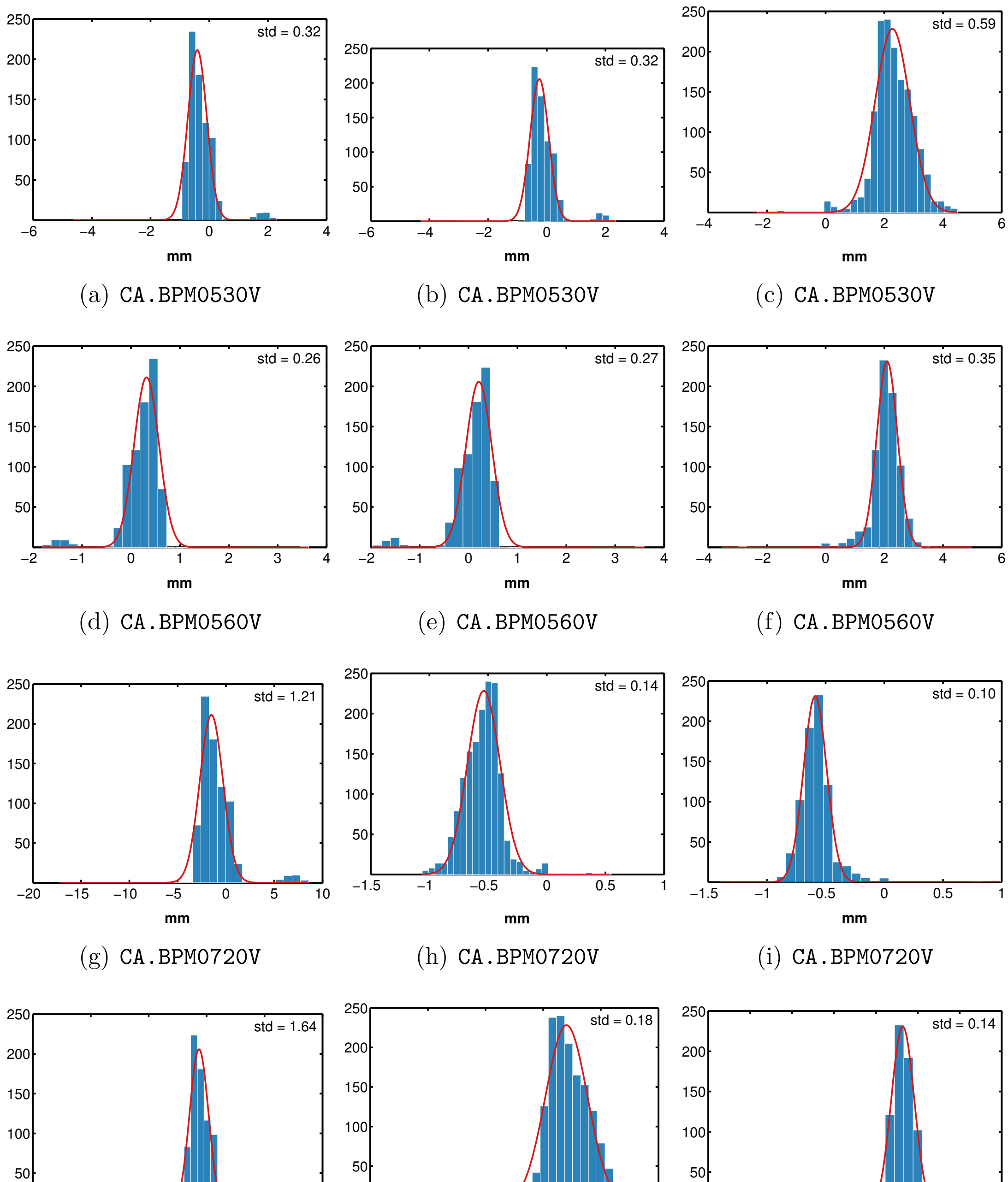

(a) `CA.BPM0530V` (b) `CA.BPM0530V` (c) `CA.BPM0530V`

(d) `CA.BPM0560V` (e) `CA.BPM0560V` (f) `CA.BPM0560V`

(g) `CA.BPM0720V` (h) `CA.BPM0720V` (i) `CA.BPM0720V`

(j) `CA.BPM0750V` (k) `CA.BPM0750V` (l) `CA.BPM0750V`

Figure 7: Resolution of the vertical probe beam BPMs calculated taking the beam position sample-by-sample along a BPM trace. Histograms of residuals between expected and measured beam position at each probe beam BPM based on the measurements of the BPM listed in the last column of Table 4 (data from 18 June 2012). The standard deviation `std` quoted at the top right of each histogram is the width of the Gaussian function fit to each distribution.

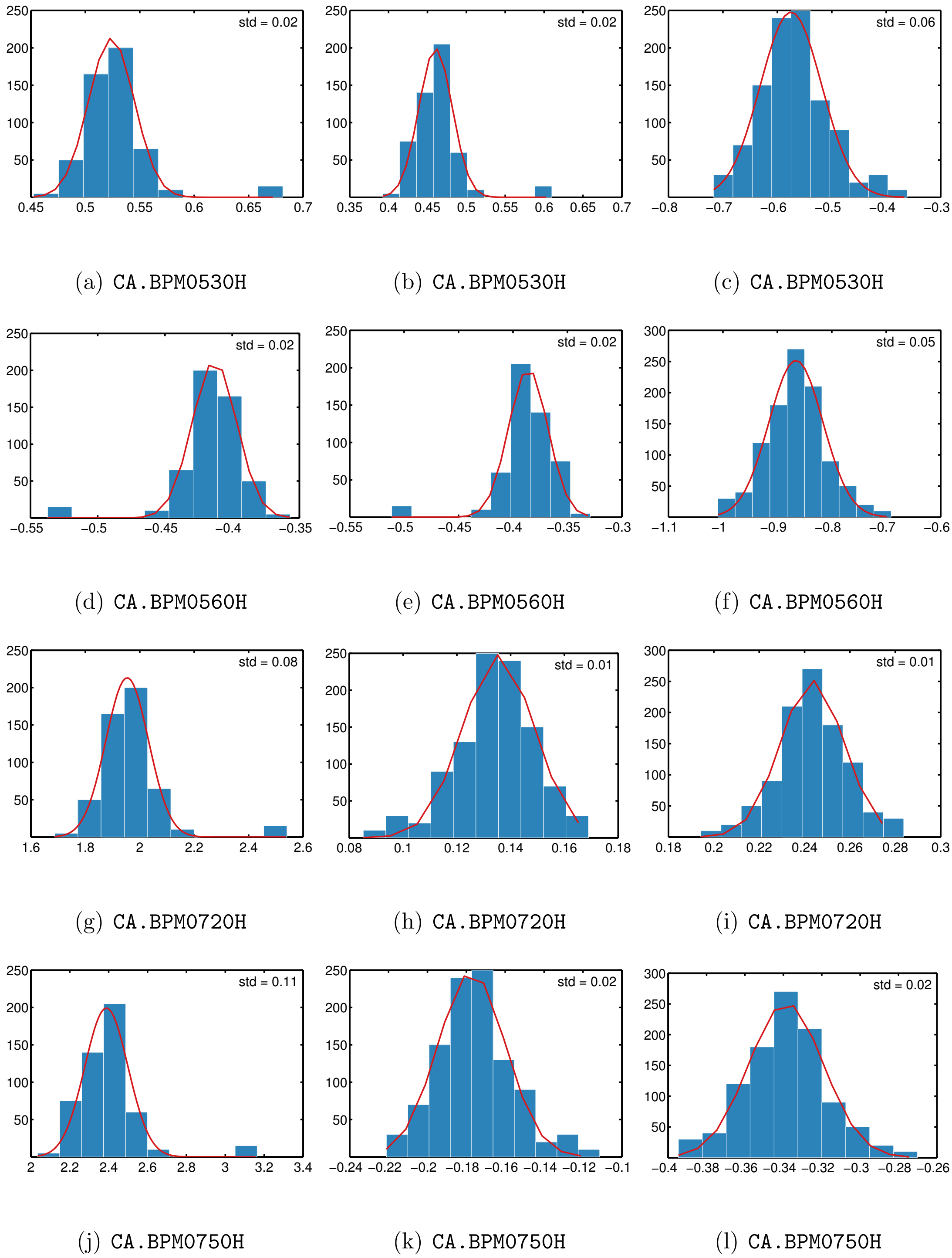

(a) `CA.BPM0530H` (b) `CA.BPM0530H` (c) `CA.BPM0530H`

(d) `CA.BPM0560H` (e) `CA.BPM0560H` (f) `CA.BPM0560H`

(g) `CA.BPM0720H` (h) `CA.BPM0720H` (i) `CA.BPM0720H`

(j) `CA.BPM0750H` (k) `CA.BPM0750H` (l) `CA.BPM0750H`

Figure 8: Resolution of the horizontal probe beam BPMs calculated averaging the beam position along a BPM trace. Histograms of residuals between expected and measured beam position at each probe beam BPM based on the measurements of the BPM listed in the last column of Table 4 (data from 18 June 2012). The standard deviation `std` quoted at the top right of each histogram is the width of the Gaussian function fit to each distribution.

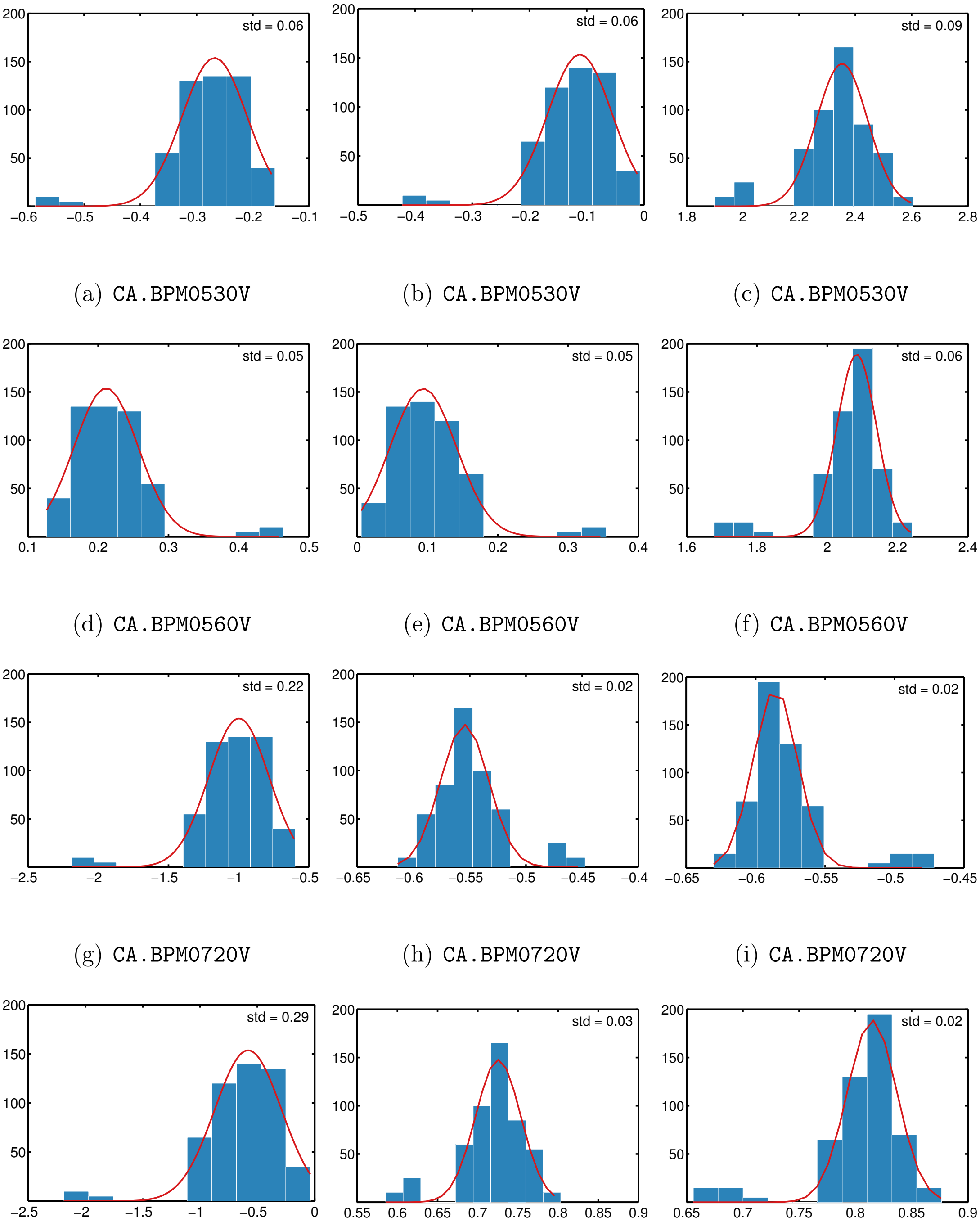

(a) `CA.BPM0530V` (b) `CA.BPM0530V` (c) `CA.BPM0530V`

(d) `CA.BPM0560V` (e) `CA.BPM0560V` (f) `CA.BPM0560V`

(g) `CA.BPM0720V` (h) `CA.BPM0720V` (i) `CA.BPM0720V`

(j) `CA.BPM0750V` (k) `CA.BPM0750V` (l) `CA.BPM0750V`

Figure 9: Resolution of the vertical probe beam BPMs calculated averaging the beam position along a BPM trace. Histograms of residuals between expected and measured beam position at each probe beam BPM based on the measurements of the BPM listed in the last column of Table 4 (data from 18 June 2012). The standard deviation `std` quoted at the top right of each histogram is the width of the Gaussian function fit to each distribution.

Table 4: Vertical and horizontal resolution of each BPM measured using the two BPM listed in the last column.

BPM Name	Resolution *sample-by-sample* Horizontal [mm]	Resolution *sample-by-sample* Vertical [mm]	Resolution *average* Horizontal [mm]	Resolution *average* Vertical [mm]	Other BPMs Used	Ref. histogram
CA.BPM0530	0.12	0.32	0.02	0.06	CA.BPM0560, CA.BPM0720	Fig. 6(a), 7(a), 8(a), 9(a)
CA.BPM0530	0.11	0.32	0.02	0.06	CA.BPM0560, CA.BPM0750	Fig. 6(b), 7(b), 8(b), 9(b)
CA.BPM0530	0.62	0.59	0.06	0.09	CA.BPM0720, CA.BPM0750	Fig. 6(c), 7(c), 8(c), 9(c)
CA.BPM0560	0.09	0.26	0.02	0.05	CA.BPM0720, CA.BPM0750	Fig. 6(d), 7(d), 8(d), 9(d)
CA.BPM0560	0.09	0.27	0.02	0.05	CA.BPM0530, CA.BPM0720	Fig. 6(e), 7(e), 8(e), 9(e)
CA.BPM0560	0.54	0.35	0.05	0.06	CA.BPM0530, CA.BPM0750	Fig. 6(f), 7(f), 8(f), 9(f)
CA.BPM0720	0.45	1.21	0.08	0.22	CA.BPM0530, CA.BPM0560	Fig. 6(g), 7(g), 8(g), 9(g)
CA.BPM0720	0.15	0.14	0.01	0.02	CA.BPM0530, CA.BPM0750	Fig. 6(h), 7(h), 8(h), 9(h)
CA.BPM0720	0.15	0.10	0.01	0.02	CA.BPM0560, CA.BPM0750	Fig. 6(i), 7(i), 8(i), 9(i)
CA.BPM0750	0.56	1.64	0.11	0.29	CA.BPM0530, CA.BPM0560	Fig. 6(j), 7(j), 8(j), 9(j)
CA.BPM0750	0.19	0.18	0.02	0.03	CA.BPM0530, CA.BPM0720	Fig. 6(k), 7(k), 8(k), 9(k)
CA.BPM0750	0.21	0.14	0.02	0.02	CA.BPM0560, CA.BPM0720	Fig. 6(l), 7(l), 8(l), 9(l)

References

[1] Marek Gasior. An inductive pick-up for beam position and current measurements. In *Proceedings DIPAC 2003*, 2003.

[2] W. Farabolini, F. Peauger, J. Barranco, S. Bettoni, B. Constance, R. Corsini, M. Csatari, S. Doebert, A. Dubrovskiy, T. Persson, G. Riddone, P. K. Skowroński, F. Tecker, D. Gudkov, A. Solodko, M. Jacewicz, T. Muranaka, R. Ruber, A. Palaia, and V. Ziemann. Two beam test stand experiments in the clex ctf3 facility. In *Proceedings of IPAC2011, San Sebastian, Spain*, pages 29 – 31, September 2011.

[3] Magnus Johnson. BPM calibration for two-beam test-stand. EDMS document 893663, CERN, June 2008.

[4] Lars Søby. Software requirements for CTF3 TL2 and CLEX BPM's. EDMS document 993952, CERN, May 2008.

[5] IEC BIPM, ILAC IFCC, IUPAP IUPAC, and OIML ISO. International vocabulary of metrology—basic and general concepts and associated terms (vim), 3rd edn. jcgm 200: 2008, 2008.

[6] B. Favrat. Schematic layout of the probe beam (CLEX). CERN Drawing Database.

[7] R. Roux. Correcteurs dipolaires de CALIFES. EDMS document 980764, CERN, December 2008.